RSC Advances

ROYAL SOCIETY OF CHEMISTRY

www.rsc.org/advances

Journal Name

ARTICLE

A pH-sensitive nanocarrier for co-delivery of doxorubicin and camptothecin to enhance chemotherapeutic efficacy and overcome the multidrug resistance in vitro

Received 00th January 20xx,
Accepted 00th January 20xx

DOI: 10.1039/x0xx00000x

www.rsc.org/

Zhen Li[a], Hongmei Li[a], Lixiang Liu[a], Xinyi You[b], Chaofeng Zhang*[b] and Yue Wang**[a]

To deliver chemotherapeutic drugs simultaneously, using drug carriers is a feasible strategy for the better synergetic effect. We have constructed a hollow silica nanoparticles (HSNPs) sealed with ZnO quantum dots (QDs) as a pH-sensitive nanocarrier, where the HSNPs have the large hollow interiors for delivering hydrophobic camptothecin (CPT) and the mesoporous structure for delivering hydrophilic doxorubicin (DOX • HCl). This cooperative drug loading has largely increased the drug encapsulation efficiency that both CPT and DOX are up to 89.28% and 44.98%, respectively. Meanwhile, the ZnO QDs lids in this drug delivery system are found to be rapidly dissolved in the acidic intracellular compartments to trigger a pH-sensitive drug releasing. The co-delivery of multi-drugs with different anticancer mechanisms in the same nanocarrier, enables the intracellular release of the drug combinations to highly enhance chemotherapeutic efficacy and overcome the multidrug resistance (MDR).

Introduction

Chemotherapy is one of the main treatments used in cancer therapy. To improve the therapeutic efficacy, efficient delivery of therapeutics into cells to increase the drug concentration is a major challenge.[1,2] Especially for the hydrophobic drugs, they are difficult to be directly used as clinical drugs owing to the poor water solubility, which may prevent them from cellular uptaking and resulting in low pharmacological bioavailability.[3-5] Among these, camptothecin (CPT) as a topoisomerase I inhibitor, is widely used against various cancers types, including colorectal, lung, cervical, and ovarian cancer via a unique mechanism of action: forming stable "Drug-Topoisomerase I-DNA" ternary complex.[6] CPT has no typical cross-resistance with other anticancer drugs and it could be used in combinational chemotherapy to overcome the drug resistance.[7-10] Nevertheless, the CPT has poor water solubility and rapid hydrolysis.[11] During circulation in-vivo, the therapeutically active lactone of CPT tends to open the lactone ring to generate the inactive and toxic carboxylate species owing to the blood weakly alkaline and contains abundant serum albumin.[12-14]

To this end, Nanoparticle (NP)-based vehicles have been developed for the drugs delivery of cancer therapeutics in order to improve the efficacy of cellular uptake, achieve the controlled drug release and drugs co-delivery.[15] Those NP-based drug delivery system (DDS) tended to increase drug accumulation in tumors through the enhanced permeability and retention effect (EPR), resulting in minimize the invasive damage to normal tissues. Among various types of nanomaterials, mesoporous silica nanoparticles (MSPs) have excellent advantages including high stability, large pore volume, high surface area, ease surface modification, tunable nanoparticle size and dosage-dependent toxcity.[16-18] In particular, hollow mesoporous silica nanoparticles (HSNPs) are superior to normal MSPs for drug delivery because the hollow cores ensure higher drug loading capability.[19-21] Besides this, the distinctive structural of the large hollow interior can function as the reservoir for hydrophobic agents, as well as the mesoporous silica shell with pore volume to guarantee efficient encapsulation of hydrophilic agents. Thus, the HSNPs achieve the simulation of organic emulsions or liposomes because of the unique nano-structure, exhibiting the simultaneously enwrap both hydropobic and

[a] Key Laboratory of Biomedical Functional Materials, School of Sciences, China Pharmaceutical University, Nanjing 211198, China. E-mail: zwy_1115@126.com
[b] Research Department of Pharmacognosy, China Pharmaceutical University, Nanjing 211198, China. E-mail: nichaofeng@126.com

hydrophilic drugs.[7,22,23] However, HSNPs always expose all of the pores that connect to the hollow interior, which may cause the loss of all of the loading out of control[24,25]. So, additional modification of HSNPs to control the delivery process is required. Hence, in our regards, we designed the HSNPs mentioned above with sealed agents to achieve the triggered releasing.

Excellent approaches for stimuli-triggered opening of the capper could be classified into the following categories, such as pH change, redox reaction, enzyme-mediated action, light irradiation, magnetic field, and temperature change and so on.[26-31] Among these, the pH-response has been extensively used for selective releasing of anticancer drugs in tumor tissues and cells. It is well known that the pH value in tumor tissues is more acidic than that in normal tissue and blood, where endosomes and lysosomes would exhibit even lower pH values.[32] The key issue for these pH-response systems is how to "switch on" and "switch off" the carriers in response to the pH signals.[33] In the literature, anchoring a polyamine onto the surface of the mesopores is limited in anticancer by their base-driven release. Other acid-responsive supramolecular nanovalves such as acetal and boronate ester is triggered at rather low pH (3-4).[34, 35]

To circumvent these challenges, ZnO quantum dots (QDs) which can be rapidly dissolved at pH lower than 5.0 but are stable at pH 7.4 are considered to be used as the lids of the nanocarrier.[36,37] When the ZnO lids through amide bond connecting with the nanoparticles outface, they could sturdy seal the nanoparticles. And the lids could easily dissolve into the cancer cells due to the acid enviroment.[36] Besides, ZnO QDs are of significant interests for bioimaging and fluorescence labelling for their excellent cellular imaging. In contrast with the traditional florescence dyes, a single light source of the QDs can be excited with the wider excitation window, which could be tuned from the ultraviolet, through the visible and near-infrared region, and even into the mid-infrared.[38, 39]

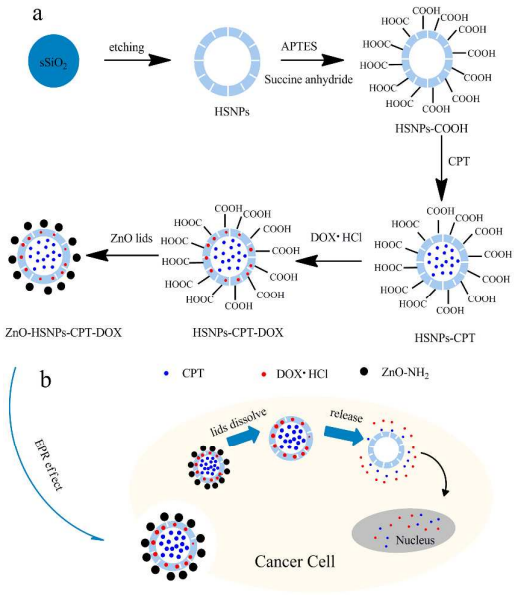

Fig.1 (a) Schematic illustration of the synthetic process of the pH-sensitive anticancer nanocarrier (ZnO-HSNPs-CPT-DOX). (b) Illustration of the ZnO lids dissolve in cancer cells for drug releasing and synergetic chemotherapeutic effect by CPT and DOX.

Among these QDs, ZnO QDs offer superior biocompatibility owing to Zn^{2+} playing a more important role in adult body as an important trace element in humans.[37,40] On the other hand, the toxicity of ZnO nanoparticles, in many cases, have been shown related to their prone dissolution in the acid circumstance[41]. The release of free Zn^{2+} is responsible for the observed toxicity, including damage to DNA via the generation of radical oxygen species (ROS)[42]. Other study also found the mechanism of ZnO nanoparticles toxicity is due to variation in dissolution kinetics[43]. Furthermore, the ZnO nanoparticles preferentially kill cancer cells owing to the cancerous T cells exhibit higher inducible levels of ROS than normal T cells[44]. But ZnO QDs have low toxicity in normal cells (MDBK) and can display potential application in cancer chemotherapy[45]. And the ZnO has a lethal dose (LD50) of 7.950 mg kg^{-1} in mice, making it relatively nontoxic[46].

Herein, in our study, we designed a novel HSNPs sealed with ZnO QDs nanocarrier as a pH-sensitive drug delivery system. It is supposed to solve the co-delivery of both hydrophobic anticancer drug CPT and hydrophilic drug DOX • HCl. We wish with high drug loading and the controlled release ability, the inhibition in vitro on the tumor cell lines can be extremely enhanced. Furthermore, the topoisomerase I inhibitor CPT, combined with the topoisomerase II inhibitor DOX • HCl, could show the encouraging bright future for overcoming the multidrug resistance (MDR) of tumors (Fig.1).

Experiment section

Materials

Chemicals and reagents were used without further purifications. Tetraethylorthosilicate (TEOS) was purchased from Alfa Aesar. Cetyltrimethylammonoiumbromide (CTAB), sodium carbonate (Na_2CO_3), absolute ethanol, sodium hydroxide (NaOH), zinc acetate, magnesium acetate, succinic anhydride, 3-aminopropyltriethoxysilane (APTES), and 1-ethyl-3-(3-dimethylaminopropyl)carbodiimide (EDC) were purchased from Sinopharm Chemical Reagent Co. (Shanghai, China). Doxorubicin • HCl (DOX • HCl) and camptothecin (CPT) were purchased from Melone Pharmaceutical Co. (Dalian, China). 3-(4,5-dimethylthiazol-2-yl)-2,5-diphenyltetrazolium bromide (MTT) were purchased from KeyGEN BioTECH (Nanjing, China). Deionized water was used in all experiments.

Characterization

Transmission electron microscopy (TEM) was performed on a JEOL-2100 with accelerating voltage of 200 kV. TEM samples were prepared by drop-casting dispersion onto copper grids covered by carbon film. Ultrathin sections for Bio-TEM were cut with a diamond knife on a Leica ultracut R ultramicrotome. The surface area, pore size, and pore-size distribution of the samples were determined by Brunauer–Emmett–Teller (BET), nitrogen adsorption–desorption and Barrett–Joyner–Halenda (BJH) methods (BEL SORPmini). The X-ray powder diffraction patterns (XRD) were recorded on an X'Pert diffractometer (Panalytical) with CuKα radiation (λ = 1.54060 Å) at 45 kV and 40 mA. Infrared spectra (4,000 to 400 cm^{-1}) were recorded on Bruker Fourier transform infrared (FT-IR) spectrometer in KBr pellets. The surface charge of the nanocarriers was investigated on Malvern Zetasizer Nano ZS 90 zeta potential analyzer. Fluorescence spectra were collected using a RF-5301 PC spectrometer. Ultraviolet-visible (UV) spectra were collected using a LAMBDA-35 spectrometer. Confocal images were acquired using a Zeiss confocal laser scanning (CLSM) unit mounted on an LSM 710 fixed-stage upright microscope.

Preparation of the solid SiO_2 nanoparticles (SP)

Solid SiO_2 nanoparticles (~100 nm) were synthesized via the method according to previous reports[47]. Fristly, TEOS (6 ml) and ammonium hydroxide (3.15 ml) were dissolved into an ethanol/deionized water (74 ml/10 ml, v/v) mixture, which was stirred at room temperature for 60 min. Then the silica particles were centrigated (10,000 rpm, 8 min) and washed with ethanol and deionized water.

Preparation of SiO_2@mSiO_2 core/shell nanoparticles

Solid SiO_2 (50 mg) nanoparticles were dispersed in distilled water by ultrasonication for 15 min. Then added with CTAB (75 mg), ammonium hydroxide (0.275 ml) into ethanol/deionized water (15 ml/15 ml, v/v) solution, stirred at room temperature for 30 min, TEOS (0.125 ml) was subsequently added to the mixture solution and kept for another 6 h. The products were collected by centrifugation (10,000 rpm, 5 min). Then, the products were re-dispersed in 15 ml of deionized water.

Preparation of hollow silica nanoparticles

A selective etching method[48] was used for the preparation of the hollow silica nanocapsules. Na_2CO_3 (212 mg) were added into the above SiO_2@mSiO_2 aqueous suspension with stirring. At this stage, the solid shpere was selectively etched by Na_2CO_3, whereas the mesoporous silica shell was protected by CTAB surfactant[49]. After the reaction was remained at 55 °C for 8 h to selectively etch the SiO_2 core, the obtained HSNPs were washed by ethanol and deionized water. To remove the CTAB, the samples were dispersed in acetone and refluxed at 85 °C for 48 h.

Preparation of carboxylic acid-functionalized HSNPs (HSNPs-COOH)

HSNPs (500 mg) were suspended in 25 mL of toluene containing 0.1 mL of APTES. The solution was stirred under nitrogen for 4 h at 50 °C to get the amine-functionalized HSNPs (HSNPs-NH_2). Then, 200 mg of HSNPs-NH_2 was added into 10 mL DMSO solution containing succinic anhydride (85 mg) and triethylamine (85 mg). The HSNPs-COOH was obtained at 50 °C for stirring 48 h. The product was recovered by centrifugation and washed with ethanol and deionized water. [50]

Preparation of ZnO QDs

The ZnO QDs was prepared by sol-gel method as reported previously[51]. Zinc acetate (440 mg) was dissolved in ethanol (30 ml) with stirring. When the solution was cooled in ice bath, the NaOH solution dissolved in hot ethanol (10 ml) was rapidly injected into the zinc acetate solution. The mixture was stirred for 6 h until the solution showed green fluorescence under the 365 nm UV lamp. Finally, heptane was used to precipitate ZnO QDs.

Preparation of amine-capped ZnO QDs

Amine-capped ZnO QDs were obtained by adding APTES (0.34 mmol) in ethanol solution. The reaction mixture was stirred at 110 °C for 15 min. After the mixture was cooled to room temperature, the amine-capped ZnO QDs was obtained.[36]

Preparation of ZnO QDs sealed HSNPs nanoparticles ZnO-HSNPs

In order to cap the HSNPs-COOH, the HSNPs-COOH powder was re-dispersed in water and then 100 mg EDC and 5 mL of amine-capped ZnO aqueous solution (5 mg mL^{-1}) were added. The mixture was stirred for another 8 h. Finally, the precipitate was centrifuged, washed several times with water (pH 7.0).

Drug loading of DOX • HCl and CPT

For drug loading, HOOC-HSNPs-CPT were prepared by dispersion of HSNPs-COOH (50 mg) into DMSO solution of CPT (12.5 ml, 2 mg ml^{-1}) for 48 h, followed by centrifugation and drying under vacuum at room temperature. Then, HOOC-HSNPs-CPT (25 mg) were dispersed into PBS solution of DOX • HCl (2 mg ml^{-1}). After stirring at room temperature for 48 h under dark conditions, the HOOC-HSNPs-CPT-DOX were obtained by centrifugation and washed with deionized water to remove the non-encapsulation DOX • HCl, then dried under vacuum at room temperature. The HOOC-HSNPs-DOX were prepared in the same way except no CPT loading.

Preparation of ZnO QDs sealed HSNPs-CPT-DOX (ZnO-HSNPs-CPT-DOX)

The HOOC-HSNPs-CPT-DOX powder was dispersed in water and then added a certain amount of EDC and amine-capped ZnO aqueous solution (5 mg mL^{-1}). The mixture was stirred for another 8 h at room temperature. Finally, the precipitate was centrifuged, washed several times with water (pH 7.0).

Drug releasing experiments of the ZnO-HSNPs-CPT-DOX

The drug releasing was investigated at 37 °C in two different media, (a) acetate buffer (pH 5.0) and (b) phosphate buffer (pH 7.4), using a dialysis bag diffusion technique. Briefly, 10 mg of ZnO-HSNPs-CPT-DOX were respectively dispersed in 5 ml of different buffer solutions and sealed in a dialysis bag (molecular weight cutoff = 3,000). The dialysis bag was submerged in 100 ml of respective buffer solutions and stirred at 37 °C for 48 h.[52,53]

Cell Culture

A549 and MCF-7/ADR cells were maintained in DMEM (Dulbecco's modified Eagles Medium) containing 10% fetal bovine serum, 100 units mL^{-1} penicillin, and 100 mg mL^{-1} streptomyc in 37 °C, 5% CO_2 in air.

Bio-TEM observations for A549 Cell

The A549 cells were incubated with 50 μg mL^{-1} ZnO-HSNPs in DMEM medium in 5% CO_2 at 37 °C for 24 h. Then, cells were washed three times with PBS and subsequently fixed with 2.5% glutaraldehyde in 0.03 M potassium phosphate buffer for at least 24 h. Cells were then washed in PBS, postfixed with 1% osmium tetroxide in sodium carboxylate buffer, washed with 0.05 mol L^{-1} maleate, and stained with 0.5% uranylacetate in maleate buffer. After washing the cells in 0.05 mol L^{-1} maleate, the cells were dehydrated in a grading series of ethanol followed by acetone, embedded in Epon, and dried in an over at 60 °C for 4 days. Ultrathin sections of approximately 50 nm thick were cut with a diamond knife on a Leica ultracut Rultramicrotome and transferred to the copper grid. The images were viewed on JEOL-2100 electron microscopy.

CLSM observation of the uptake by A549 cells

Frist, the free DOX • HCl, CPT and HOOC-HSNPs-CPT-DOX were dispersed into DMEM cell-culture media with same drug concentration. Then, DMEM (2 mL) containing DOX • HCl, CPT and HOOC-HSNPs-CPT-DOX were added into a CLSM-specific culture dish of seeded A549 cells with a cell density of 70%-80%, respectively. After co-incubation for 6 h, the cell was washed with PBS three times and the fluorescence images of cells were obtained by the CLSM. The ZnO-HSNPs were carried out in the same way except the co-incubation time is just 30 min.

MTT evaluation of the cytotoxicity of HOOC-HSNPs-CPT-DOX against A549 cells and MCF-7/ADR cells

The in vitro cytotoxicity was evaluated by the typical MTT reduction assay. To evaluate the cytotoxicity of HOOC-HSNPs-CPT-DOX against A549 cancer cells, A549 cells were seeded in a 96-well plate at a density of 5×10^3 per well and cultured in 5% CO_2 at 37 °C for 48 h. Free DOX • HCl, HOOC-HSNPs-DOX, and HOOC-HSNPs-CPT-DOX were dispersed into DMEM with the equivalent DOX • HCl concentration by ultrasonic treatment, and the cells were incubated in 5% CO_2 at 37 °C for 48 h. And the free ZnO-HSNPs were evaluated at the concentration of 300 μg ml^{-1}. After the incubation, 20 μL of MTT solutions were added for another 4h. Then the medium solution was replaced by 150 μL DMSO solution. After 10 min, the optical density at 490 nm (absorption value) of each well was measured on a Tecan Infinite M 200 monochromator-based multifunction microplate reader. The cells only cultured with DMEM under the same condition were used as control. The cytotoxicity of the DOX • HCl, HOOC-HSNPs-DOX, and HOOC-HSNPs-CPT-DOX against MCF-7/ADR was tested in the same way as above method.

Results and Discussion

The above mentioned nanoparticles are fully characterized by (TEM). As shown in Fig.2, The uniform diameter of the HSNPs is around 180 nm and a shell thickness is nearly 28 nm (Fig.2b-c). The higher brightness of the core part is due to removal of the internal silica materials which is shown in Fig.2a. The diameter of the ZnO QDs is about 3-4 nm with a reasonably narrow size distribution and have a good dispersion（Fig.2d）, and the HRTEM image of ZnO QDs show the lattice fringes with distances of 0.26 nm (Fig.2e), which corresponds to the distance between two (002) planes of hexagonal ZnO phase[54]. The TEM images also verify the ZnO QDs successful sealing with the HSNPs. Comparing with the pure HSNPs（Fig.2b）, the distinctive darkness of the whole particles could be caused by the ZnO QDs capping (Fig.2f).

The BET surface areas measurement of HSNPs is 629 $m^2 g^{-1}$, and the BJH pore sizes distribution of HSNPs is 2.4 nm, meaning that the specific surface area is dominated by the mesoporous structure. The pore size is determined by the alkykl chain length of the

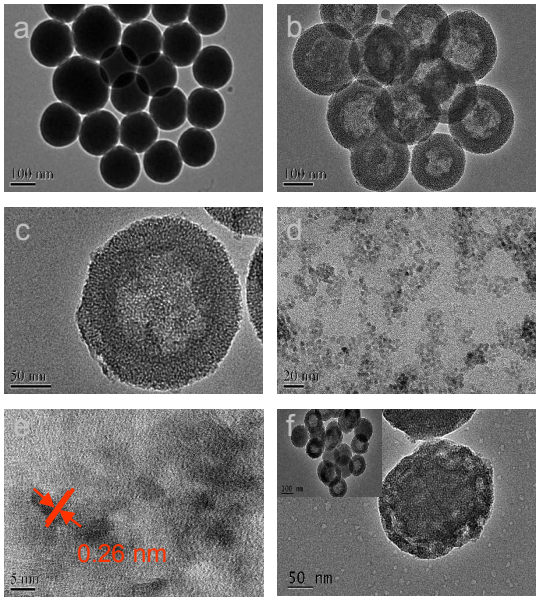

Fig.2 (a) TEM images of SiO_2 (b) and (c) Low- and high-images of HSNPs nanospheres, (d) and (e) TEM and HRTEM images of the ZnO ODs, (f) TEM image of ZnO-HSNPs (pH=7.4), insert: TEM image of ZnO-HSNPs at pH 5.0.

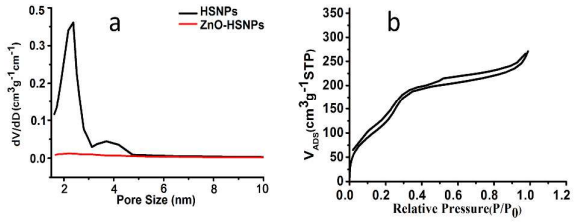

Fig.3 (a) The pore size distribution curve of HSNPs (Black) and ZnO-HSNPs (Red). (b) N_2 adsorption isotherm of HSNPs.

surfactant CTAB. The diameter of ZnO QDs is large enough to block the pores of HSNPs, thus may inhibit the release of the loaded drug. After sealed with ZnO QDs, the BJH pore sizes of nanoparticles decreased clearly which indicated that the ZnO QDs capped all of the pores of the HSNPs (Fig.3a). Type IV isotherm curves of nanoparticles further prove the successful formation of the mesoporous structures (Fig.3b). So, loading and releasing of drug molecules could be achieved through the mesoporous channels, and the hollow space could ensure a high drug-loading capacity.

As shown in Fig.4, zeta potential of pure solid SiO_2 is about -33.8 mv. After selective etching, the HSNPs, HSNPs-NH_2 and HSNPs-COOH is changing to -25.6 mv, 24.5 mv and -33.2 mv, respectively, implying the group modification is successfully completed. After thecarboxylic acid-functionalized, the mesoporous surface of the nanoparticles become electronegative. Therefore, the efficient hydrophilic drug loading could be carried out through the electrostatic interactions. Zeta potential has also shown the ZnO QDs changed from -8.9 mv to 21.7 mv after amine-capped of ZnO QDs, which clearly establish the presence of amine group anchored to the ZnO QDs via hydrolysis of APTES.

As shown in FT-IR spectrum of amine-capped ZnO QDs (Fig.5a), a broad absorption band at 3414 cm^{-1} should be attributed to the

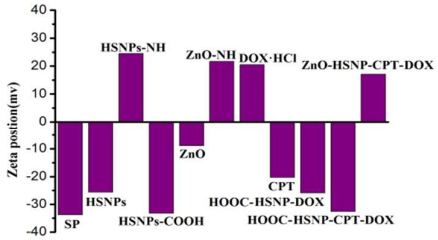

Fig.4 Zeta potential of the SP, HSNPs, HSNPs-NH_2, HSNPs-COOH, ZnO QDs, ZnO-NH_2, DOX • HCl, CPT, HOOC- HSNPs-DOX, HOOC-HSNPs-CPT-DOX and ZnO-HSNPs-CPT-DOX.

stretching band about N-H and O-H. The peak at 1587 cm^{-1} and 1408 cm^{-1} may be according to the bending vibration of N-H and C-H. The band of 1022 cm^{-1} should be due to the Si-O bond stretching vibration, and the band of 464 cm^{-1} may belong to the Zn-O bond stretching vibration, thus further confirms ZnO QDs have been successful amined.[55] Appearance of a wide and weak peak located at 2 θ = 22 ° further confirmed the presence of HSNPs with ZnO QDs and demonstrated the amorphous silica (Fig.5b).[56] As we expected, the amine-capped ZnO QDs are tested to be soluble in the water (pH=7.0). The solubility may be attributed to the exposed hydrophilic group such as -NH_2 and -OH.

The function of ZnO QDs lids is evidenced by the fluorescence spectroscopy (Fig.6a). As we see, with a significant UV emission peak at 365 nm, the amine-capped ZnO shows a broad green emission peak at 550 nm[36]. This result further confirms the successful synthesis of the ZnO QDs and shows that the amined ZnO QDs can play a role in tracking the delively system upon excitation at 365 nm. Amine-capped ZnO QDs are stable in the PBS solution of pH=7.4, so the florescence intensity seems very strong. But when it is dispersed in the PBS solution of pH=5.0, the florescence is completely quenched. This phenomenon verifies that the ZnO QDs can be fully dissolved at acidic condition. It is coinciding with the Fig.2f (insert) image that the ZnO QDs sealed HSNPs have smoothing surfaces in PBS (pH=5.0) because of the disintegration of ZnO QDs. The results suggest that upon internalization by cells, the ZnO QDs would dissolve in cancer internalization compartments,

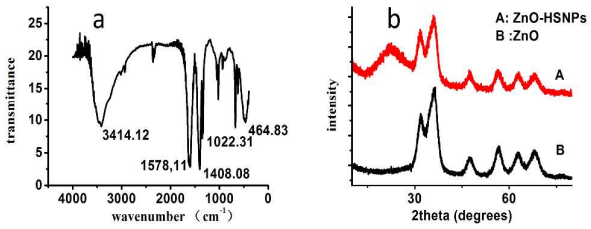

Fig.5 (a) FTIR spectra of ZnO-NH_2. (b) Wide-angle XRD patterns of ZnO QDs (Black) and ZnO-HSNPs (Red).

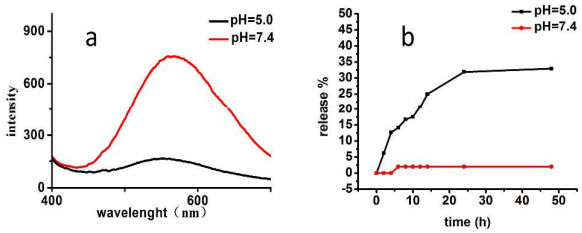

Fig.6 (a) Photoluminescence spectra of ZnO QDs at pH 7.4 (Red) and at pH 5.0 (Black), γ_{exc}=365 nm. (b) Release profiles of ZnO-HSNPs-CPT-DOX at pH 7.4 (Red) and 5.0 (Black) at 37 °C.

whereas there is little release in normal tissue. By this way, the ZnO QDs lids on HSNPs could be efficiently dissolved in the acidic intracellular compartments of cancer cell, then trigger the release of the drug cargo from the pores of the HSNPs into the cytosol, which would reduce the drug toxicity on normal cells.

Multi-drug combined chemotherapy has increasingly become a versatile strategy of great significance in clinical disease therapy because the encapsulation of multiple drugs into one system could bring forth enhanced therapeutic effect.[57] However, it has rarely been used in inorganic material systems.[7] We used hydrophilic anticancer drug DOX • HCl and the hydrophobic drug CPT as the model drugs to prove the superiority of the HSNPs over conventional MSNs.

After removal unbound DOX • HCl and CPT, the co-delivery drug system HOOC-HSNPs-CPT-DOX is formed. The CPT may tend to be encapsulated in the hollow core owing to the hydrophobic interaction. Because of the large hollow interior, highly efficient encapsulation of the CPT is extremely guaranteed. And the DOX • HCl may tend to deposit in the mesoporous shell of HSNPs and bind tightly via electrostatic interactions between the electropositive DOX • HCl daunosamine moiety and the electronegative carboxyl groups of the carboxylic acid-functionalized mesoporous shell of HSNPs-COOH. Thus, the DOX • HCl loading content could also be greatly enhanced.

The Zeta potential has demonstrated the perfect drug loading. As shown in Fig.4, the Zeta potential of pure DOX • HCl is about 20.5 mv. After loading DOX, the potential of HSNPs-DOX has changed to -25.9 mv, which becomes more positive than the pure HSNPs-COOH. For the zeta potential of CPT is -29.3 mv, hence, the zeta potential has changed to more negativity after loading the CPT. Furthermore, when the ZnO QDs capping onto the HOOC-HSNPs-CPT-DOX, the zeta potential of ZnO-HSNPs-CPT-DOX has increased to 17.1 mv, owing to amine-capped ZnO QDs with the positive electricity. The encapsulation efficiency of the CPT and the DOX • HCl have been measured by the UV, to be as high as 89.28% and 44.98%, respectively. Such dual-drug encapsulation with the high drug loading capacity has been rarely reported in mesoporous silica nanoparticles and other types of inorganic material systems.

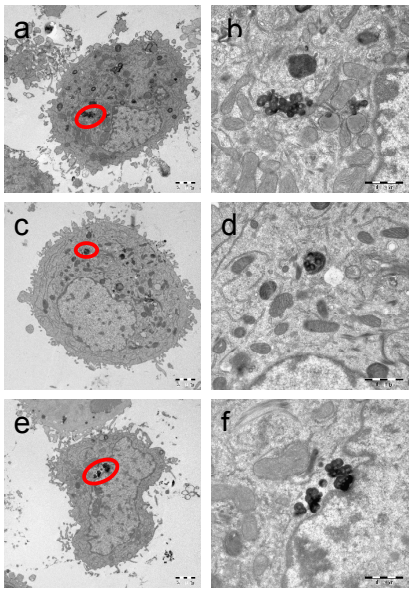

Fig.7 (a), (c) and (e) TEM images of A549 cells incubated with ZnO-HSNPs (concentration: 50 ug ml^{-1}) for 6 h, (b), (d) and (f) is the corresponding enlarged scale.

The DOX • HCl release from the ZnO-HSNPs-CPT-DOX nanoparticles against buffer solution at pH=5.0 and pH=7.4 was studied to simulate a cellular lysosome environment and a normal physiological environment. At pH=5.0, the DOX • HCl release reaches up to 32.93% which is within the reasonable range of the reported case, [37,58] due to the disintegration of the ZnO QDs and the impairment of the electrostatic interaction of DOX • HCl with COO^-, as well as enhancement of the releasing of DOX under acidic conditions. However, the drug release at pH 7.4 is really limited within 24 h, indicating that ZnO QDs have a well protection from the drug releasing in normal tissues (Fig.6b).

Bio-TEM was used to observe the cell morphologies and the specific location of the endocytosed ZnO-HNSPs nanocarrier within A549 cells. It is observed that A549 cells treated with the ZnO-HSNPs keep intact structures of cell membrane and nucleus (Fig.7 a-b). It means that ZnO-HNSPs are non-cytotoxic under the current conditions. From the enlarged image Fig 7b, some HSNPs particles are found to aggregate in the cytoplasm, even still keeping their perfect core-shell structure. And we can see clearly that the ZnO-HSNPs escape from the endosome via cellular “sponge effects” (Fig7 c-d), and enter the cytoplasm of cancer cells (Fig.7e-f).

To better understand the interactions between the nanocarrier and cancer cells in vitro, we use the CLSM to trace the distribution of the HSNPs in the cell. As shown in Fig.8, the efficient uptake of the ZnO-HSNPs by A549 cells can be clearly observed from the green fluorescence emission of the ZnO QDs. The intensity of the green fluorescence from ZnO QDs is a little bit weak, because of the dissolution of the QDs in acidic cancer cells[59]. From the images we find the fluorescence is just distributed around the nucleus, which indicates that the HSNPs can enter into the cytoplasm but be kept from the nucleus.

The fluorescent nature of CPT (blue fluorescence) excited at 365 nm and DOX (red fluorescence) excited at 488 nm molecules facilitates the in situ observation of intracellular delivery and release of drugs from the carriers. As shown in Fig.9, the red and blue fluorescence appear simultaneously in the A549 cancer cells

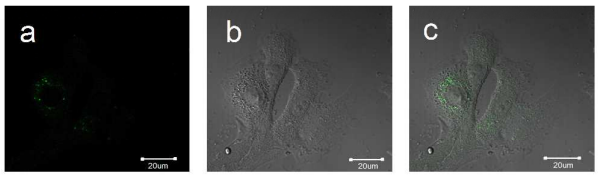

Fig.8 CLSM images of A549 cells incubated with ZnO-HSNPs (concentration: 50 ug ml^{-1}) for 30 min. (a) ZnO channel, (b) bright field channel, (c) Merge of (a) and (b).

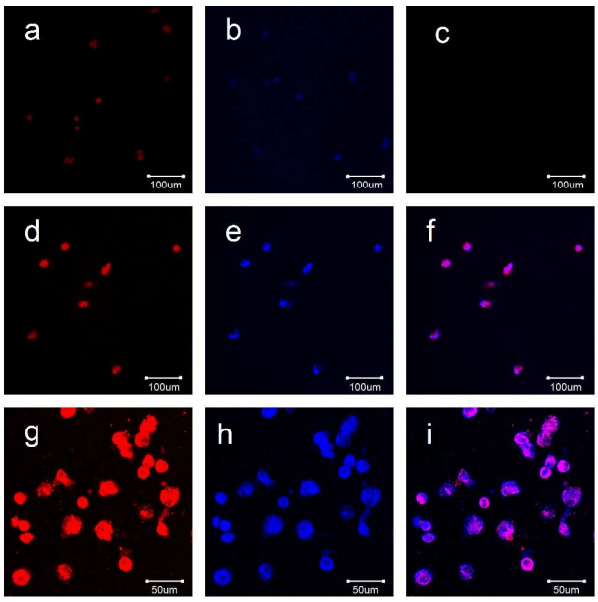

Fig.9 CLSM images (a) of A549 cells incubated with free DOX (concentration: 5 ug ml^{-1}) for 6 h, (b) of A549 cells incubated with free CPT (concentration: 8 ug ml^{-1}) for 6 h, (c) control. Images (d)-(i) of A549 cells incubated with HOOC-HSNPs-CPT-DOX (DOX concentration: 5 ug ml^{-1}) for 6 h (d) and (g) DOX channel, (e) and (h) CPT channel, (f) and (i) Merge of the DOX and CPT channel.

after 6 h co-incubation, and the pink fluorescence in the merged images of the red and blue demonstrates that HSNPs could operate an intracellular co-delivery of DOX • HCl and CPT from the CLSM images. Compared to the free DOX • HCl and CPT drugs (Fig.9a-b), the fluorescent intensity of the HOOC-HSNPs-CPT-DOX has increased obviously. It indicates that HSNPs have greatly improved the cellular uptake compared to the free drug. And we find after incubation 6 h, the drug fluorescence is mainly distributed in the nucleus from CLSM images (Fig.9d-i), indicating that DOX • HCl and CPT could be released in the cytoplasm and then enter the nucleus afterwards.

To investigate the enhanced therapeutic effect caused by the co-delivery of the two drugs, the MTT assay was adopted to assess the cytotoxicity of free DOX • HCl, HOOC-HSNPs-DOX, HOOC-HSNPs-CPT-DOX and the free ZnO-HSNPs. It was found that the ZnO-HSNPs nanocarrier exhibits no appreciable negative effect on the viability of cells. The cells viability is nearly 95.1% even at high concentration up to 300 μg ml^{-1}, which proves that the ZnO-HSNPs have the good biocompatibility.

As shown in Fig.10a, free DOX • HCl, HOOC-HSNPs-DOX, HOOC-HSNPs-CPT-DOX have obvious cytotoxicity in A549 cells, and they all show an increasing concentration dependent inhibition against A549. By comparison with the free DOX • HCl, much more DOX • HCl is taken in and then released inside cell to induce cell death by the HOOC-HSNPs-DOX, thus the latter shows higher cytotoxicity than free DOX • HCl under the equivalent conditions. At low drug concentrations, there is no obviously change between free drug and HOOC-HSNPs-DOX. Take the DOX • HCl concentration as standard, once the concentration up to the 5 μg ml^{-1}, the cell viabilities incubation with the HOOC-HSNPs-DOX is 27.95%, which is decrease nearly half of 53.51% compared to the free DOX • HCl. When the DOX • HCl concentration is increased to 10 μg ml^{-1}, the cell viabilities incubation alter more clearly which is decrease 43.43% to 20.09%, respectively. It is not surprising that the combination of the two drugs shows a better inhibition activity for cancer cells than the individual drug.[8] Even the drug concentration is low to 1.25 μg ml^{-1}, the cell viabilities of HOOC-HSNPs-CPT-DOX is 30.46%, which is nearly equal to the HOOC-HNSPs-DOX at the DOX • HCl concentration of 5 μg ml^{-1}. Thus, CPT and DOX • HCl are playing a part of synergistic inhibitory activity in the same nanocarrier. This co-delivery nanocarrier could circulate within the blood vessel and penetrate into the tumor tissue by the enhanced EPR effect and enhanced the chemotherapeutic afterward.

In order to investigate whether this co-delivery system could overcome the multidrug resistance of cancer cells, we carry out it against MCF-7/ADR cell line. The MCF-7/ADR cells really exhibit a high drug resistance to the DOX molecules, demonstrated by the lower cytotoxicity of free DOX • HCl against MCF-7/ADR cells. As shown in Fig.10b, when the concentration of the free DOX • HCl up to 20 μg ml^{-1}, the cell viabilities still reach up to 68.89%. When the DOX • HCl was encapsulated into the HSNPs, the cytotoxic effect of

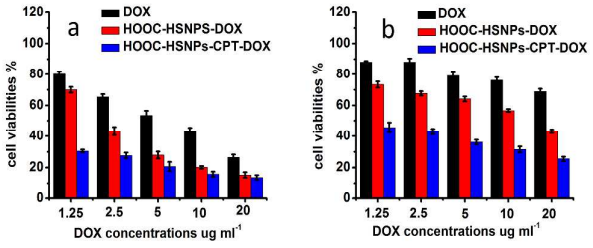

Fig.10 Cell viabilities of free DOX, HOOC-HSNPs-DOX, HOOC-HSNPs-CPT-DOX against A549 cells (a) for 48 h intervals, and MCF-7/ADR cells (b) for 48 h intervals. The error bars in the graph represent standard deviations (n = 6).

HOOC-HSNPs-DOX has been enhanced. The over-expression of multidrug efflux pumps such as P-glycoprotein (P-gp) is considered to be the main reason responsible for the drug-resistance of cancer cells.[60,61] Here, HSNPs could bypass the P-gp induced efflux action because nano-sized HSNPs are expected to be too large to be effused by P-gp.[62-64] But there is no obviously change as we see Fig.10b due to the resistance of the DOX • HCl. In addition,combination of CPT could effectively overcome the DOX resistance of MCF-7/ADR cells. The anticancer efficiency of the HOOC-HSNPs-CPT-DOX is up to 54.4 % (even at the very low DOX concentration of 1.25 μg ml^{-1}) after 48 h incubation, much higher than the free DOX • HCl and HOOC-HSNPs-DOX. This enhanced anticancer effect may be caused by the CPT with the unique mechanism of action: forming stable "Drug-Topoisomerase I-DNA" ternary complex, which is easily avoiding the development of multidrug resistance.

In summary, for the future application, the co-delivery anticancer drug can be replace to the combinations of targeting moiety, therapeutic gene, energy and the contrast agent and so on[65]. Such strategies will endow them with highly efficient to overcome the MDR and have a great application potentials for cancer therapy.

Conclusions

In summary, we have constructed a novel pH sensitive nanocarrier to co-deliver hydrophobic and hydrophilic drugs. The ZnO QDs (~3-4 nm) lids allow the high sensitivity, non-toxic and long-term stability up to several months. Before internalization into the cancer cells, the ZnO QDs could prevent drug from leaking by sealing the pores. After that, when the ZnO QDs are efficiently dissolved in the acidic intracellular compartments of cancer cells, it will trigger the release of the drug cargo from the pores of the nanocarrier into the cytosol. So, the ZnO QDs lids could allow the pH-sensitive drug release to minimize the toxicity for normal tissues. The unique structure of the HSNPs could complete the simultaneous loading of the hydrophobic drug CPT and hydrophilic drug DOX • HCl, and ensure the high drug encapsulation efficiency at the meantime. More important, different anticancer mechanism of two anticancer drugs combination could highly improve the chemotherapeutic effect and overcome the multidrug resistance of cancer cells, which make them with great clinical application potentials.

Acknowledgements

This study was sponsored by the National Natural Science Foundation of China (no. 21401216) and the Fundamental Research Funds for the Central Universities. This work was also supported by Qing Lan Project in Jiangsu Province.

Notes and references

1 B. A. Chabner and T. G. Roberts Jr., *Nat. Rev. Cancer*, 2005, **5**, 65-72.
2 D. Peer, J. M. Karp, S. Hong, O. C. Farokhzad, R. Margalit and R. Langer, *Nat. Nanotechnol.*, 2007, **2**, 751-760.
3 S. De Koker, R. Hoogenboom and B. G. De Geest, *Chem. Soc. Rev.*, 2012, **41**, 2867-2884.
4 N. J. Farrer, J. A. Woods, L. Salassa, Y. Zhao, K. S. Robinson, G. Clarkson, F. S. Mackay and P. J. Sadler, *Angew. Chem.*, 2010, **122**, 9089-9092.
5 T. L. Doane and C. Burda, *Chem. Soc. Rev.*, 2012, **41**, 2885-2911.
6 M. E. Wall, M. C. Wani, C. E. Cook, K. H. Palmer, A. T. McPhail and G. A. Sim, *J. Am. Chem. Soc.*, 1966, **88**, 3888-3890.
7 Y. Chen, Y. Gao, H. R. Chen, D. P. Zeng, Y. P. Li, Y. Y. Zheng, F. Q. Li, X. F. Ji, X. Wang, F. Chen, Q. J. He, L. L. Zhang and J. L. Shi, *Adv. Funct. Mater.*, 2012, **22**, 1586-1597.
8 L. M. Zhang, J. G. Xia, Q. H. Zhao, L. W. Liu, and Z. J. Zhang, *small*, 2010, **6**, 537-544.
9 M. Andersson, E. Lindegaard Madsen, M. Overgaard, C. Rose, P. Dombernowsky and H. T. Mouridsen, *Eur. J. Cancer*, 1999, **35**, 39-46.
10 V. Gavrilov, M. Steiner and S. Shany, *Anticancer Res.*, 2005, **25**, 3425-3429.
11 C. J. Thomas, N. J. Rahier and S. M. Hecht, *Bioorg. Med. Chem.*, 2004, **12**, 1585-1604.
12 Q. Q. Zhang, J. L. He, M. G. Zhang and P. H. Ni, *J. Mater. Chem. B*, 2015, **3**, 4922-4932
13 J. F. Pizzolato and L. B. Saltz, *Lancet*, 2003, **361**, 2235-2242.
14 Q. Y. Li, Y. G. Zu, R. Z. Shi and L. P. Yao, *Curr. Med. Chem.*, 2006, **13**, 2021-2039.
15 Y. Pan, H. Bao, N. G. Sahoo, T. Wu and L. Li, *Adv. Funct. Mater.*, 2011, **21**, 2754-2763.
16 F. Tang, L. Li and D. Chen, *Adv. Mater.*, 2012, **24**, 1504-1534.
17 C. Chen, J. Geng, F. Pu, X. Yang, J. Ren and X. Qu, *Angew. Chem., Int. Ed.*, 2011, **50**, 882-886.
18 H. Meng, W. X. Mai, H. Y. Zhang, M. Xue, T. Xia, S. J. Lin, X. Wang, Y. Zhao, Z. X. Ji, J. I. Zink and A. E. Nel, *Acs Nano*, 2013, **7**, 994-1005.
19 I. I. Slowing, J. L. Vivero-Escoto, C.-W. Wu and V. S.-Y. Lin, *Adv. Drug Deliv. Rev.*, 2008, **60**, 1278-1288.
20 R. Anand, M. Malanga, I. Manet, F. Manoli, K. Tuza, A. Aykac, C. Ladaviere, E. Fenyvesi, A. Vargas-Berenguel, *R. Gref and S. Monti, Photochem. Photobiol. Sci.*, 2013, **12**, 1841-1854.
21 P. Yang, S. Gai and J. Lin, *Chem. Soc. Rev.*, 2012, **41**, 3679-3698.
22 Y. Chen, C. Chu, Y. C. Zhou, Y. F. Ru, H. R. Chen, F. Chen, Q. J.He, Y. L. Zhang, L. L. Zhang and J. L. Shi, *Small*, 2011, **7**, 2935-2944.
23 Y. Chen, H. R. Chen, D. P. Zeng, Y. B. Tian, F. Chen, J. W. Feng and J. L. Shi, *ACS Nano*, 2010, **4**, 6001-6013.
24 L. Du, S. Liao, H. A. Khatib, J. F. Stoddart and J. I. Zink, *J. Am. Chem. Soc.*, 2009, **131**, 15136-15142.
25 J. Zhang, Z. F. Yuan, Y. Wang, W. H. Chen, G. F. Luo, S. X. Cheng, R. X. Zhuo and X. Z. Zhang, *J. Am. Chem. Soc.*, 2013, **135**, 5068-5073.
26 W. Chen, P. Zhong, F. Meng, R. Cheng, C. Deng, J. Feijen and Z. Zhong, *J. Controlled Release,* 2013, **169**, 171-179.
27 R. Guo, L. L. Li, W. H. Zhao, Y. X. Chen, X. Z. Wang, C. J. Fang, W. Feng, T. L. Zhang, X. Ma, M. Lu, S. Q. Peng and C. H. Yan, *Nanoscale*, 2012, **4**, 3577-3583.
28 T.-W. Kim, I. I. Slowing, P.-W. Chung and V. S.-Y. Lin, *ACS Nano*, 2010, **5**, 360-366.
29 C. H. Lee, S. H. Cheng, I. Huang, J. S. Souris, C. S. Yang, C. Y. Mou and L. W. Lo, *Angew. Chem.*, 2010, **122**, 8390-8395.
30 C. Park, H. Kim, S. Kim and C. Kim, *J. Am. Chem. Soc.*, 2009, **131**, 16614-16615.

31 H. Yan, C. Teh, S. Sreejith, L. Zhu, A. Kwok, W. Fang, X. Ma, K. T. Nguyen, V. Korzh and Y. L. Zhao, *Angew. Chem., Int. Ed.*, 2012, **51**, 8373-8377.
32 J. Z. Du, X. J. Du, C. Q. Mao and J. Wang, *J. Am. Chem. Soc.*, 2011, **133**, 17560-17563.
33 Z. Luo, X. W. Ding, Y. Hu, S. J. Wu, Y. Xiang, Y. F. Zeng, B. L. Zhang, H. Yan, H. C. Zhang, L. L. Zhu, J. J. Liu, J. H. Li, K. Y. Cai and Y. L. Zhao, *ACS Nano*, 2013, **7**, 10271-10284.
34 T. D. Nguyen, K. C.-F. Leung, M. Liong, C. D. Pentecost, J. F. Stoddart, J. I. *Zink, Org. Lett.*, 2006, **8**, 3363–3366.
35 R. Liu, Y. Zhang, X. Zhao, A. Agarwal, L. J. Mueller and P. Feng, *J. Am. Chem. Soc.*, 2010, **132**, 1500-1501.
36 F. H. Muhammad, M. Y. Guo, W. X. Qi, F. X. Sun, A. F. Wang, Y. J. Guo, and G. S. Zhu, *J. Am. Chem. Soc.*, 2011, **133**, 8778-8781.
37 S. Wu, X.Huang and X. Du, *J. Mater. Chem. B*, 2015, **3**, 1426-1432.
38 S. Weiss, M. Bruchez, M. Moronne, P. Gin and AP. Alivisatos, *Science*, 1998, **281**, 2013-2016.
39 J. M. Li, Y. Y. Wang, M. X. Zhao, C. P. Tan, Y. Q. Li, X. Y. Le, L. N. Ji and Z. W. Mao, *Biomaterials*, 2012, **33**, 2780-2790
40 J. H. Henzel, M. S. DeWeese and E. L. Lichti, *Arch. Surg.*, 1970, **100**, 349–357.
41 T. Xia, M. Kovochich, M. Liong, L. Madler, G. Gilbert, H. Shi, J. I. Yeh, J. I. Zink and A. E. Nel, *ACS Nano*, 2008, **2**, 2121-2134.
42 I. G. Gazaryan, I. P. Krasinskaya, B. S. Kristal and A. M. Brown, *J. Biol. Chem.*, 2007, **282**, 24373-24380.
43 H. Yang, C. Liu, D. Yang, H. Zhang and Z. Xi, *J. Appl. Toxicol.*, 2009, **29**, 69-78.
44 C. Hanley, J. Layne, A. Punnoose, K. M. Reddy, I. Coombs, A. Coombs, K. Feris and D. Wingett, *Nanotechnology*, 2008, **19**, 295103-295113.
45 Z. Fakhroueian, A. M. Dehshiri, F. Katouzian and P. Esmaeilzadeh, *J. Nanopart Res.*, 2014, **16**, 2483-2897.
46 S. Arora, J. M. Rajwade and K. M. Paknikar, *Toxicol. Appl. Pharmacol.*, 2012, **2**, 151-165.
47 G. Qi, Y. Wang, L. Estevez, A. K. Switzer, X. Duan, X. Yang and E. P. Giannelis, *Chem. Mater.*, 2010, **22**, 2693–2695.
48 X. Fang, C. Chen, Z. Liu, P. Liu and N. Zheng, *Nanoscale*, 2011, **3**,1632-1639.
49 X. Ma, Y. Zhao, K. W. Ng, and Y. L. Zhao, *Chem. Eur. J.*, 2013, **19**, 15593-15603.
50 F. D. Juan and E. Ruiz-Hitzky, *Adv. Mater.*, 2000, **12**, 430-432.
51 J. Bang, H. Yang and P. H. Holloway, *Nanotechnology*, 2006, **17**, 973-978.
52 J. Bang, H. Yang, P. H. Holloway, D. Chen, X. Teng and J. Q. He, *ACS Nano*, 2010, **4**, 6874-6882.
53 C. Y. Yang, W. Guo, L. R. Cui, N. An, T. Zhang, H. M. Lin and F. Y. Qu, *Langmuir*, 2014, **30**, 9819-9827.
54 D. I. Son, B. W. Kwon, D. H. Park, W. S. Seo, Y. Yi, B. Angadi, C.-L. Lee and W. K. Choi, *Nat. Nanotechnol.*, 2012, **7**, 465-471.
55 N. Uekawa, N. Mochizuki, J. Kajiwara, F. Mori, Y. J. Wu and K. Kakegawa, *Phys. Chem. Chem. Phys*, 2003, **5**, 929-934.
56 S. Kumar, A. Daverey, N. K. Sahu and D. Bahadur, *J. Mater. Chem. B*, 2013, **1**, 3652-3660.
57 S. M. Lee , T. V. O'Halloran and S. T. Nguyen , *J. Am. Chem. Soc.*, 2010, **132**, 17130-17138.
58 D. D. Wang, Z. G. Xu, Z. J. Chen, X. Y. Liu, C. L. Hou, X. Y. Zhang and H. X. Zhang, *ACS Appl. Mater. Interfaces*, 2014, **6**, 12600-12608.
59 A. Goux, T. Pauporte, J. Chivot and D. Lincot, *Acta*, 2005, **50**, 2239-2248.
60 Y. D. Livney and Y. G. Assaraf, *Adv. Drug Deliv. Rev.*, 2013, **65**, 1716-1730.
61 L. S. Jabr-Milane, L. E. van Vlerken, S. Yadav and M. M. Amiji, *Cancer Treat. Rev.*, 2008, **34**, 592-602.
62 C. M. J. Hu and L. F. Zhang, *Biochem. Pharmacol.*, 2012, **83**, 1104-1111.
63 Z. B. Gao, L. N. Zhang and Y. J. Sun, *J. Controlled Release*, 2012, **162**, 45-55.
64 C. S. Kim, G. Y. Tonga, D. Solfiell and V. M. Rotello, *Adv. Drug Deliv. Rev.*, 2013, **65**, 93-99.
65 Y. Chen, H. R. Chen and J. L. Shi, *Mol. Pharmaceutics*, 2014, **11**, 2495-2510